

RESEARCH

Open Access



On the performance of the Code Division Duplex system using interference rejection codes

Yufang Yin¹, Gangjun Li¹, Li Li² and Hua Wei^{2*}

Abstract

In this paper, we investigate the performance of the Code Division Duplex (CDD) system using the interference rejection codes, which exhibit zero correlation values on the relative delay-induced code offsets and can be applied to mitigate the mutual interference between the uplink and downlink. Specifically, we propose to employ loosely synchronous codes to effectively combat the interference through the interference-free window. Moreover, the simplified RAKE structure is proposed as the receiver of the CDD device, which can significantly reduce the complexity in the implementation. The simulation results demonstrate that our proposed method can achieve a near interference-free performance when the user load of the system is moderate.

1 Introduction

A duplex communication system [1] is a point-to-point system composed of two connected parties or devices that can communicate with one another in both directions, normally termed as uplink and downlink individually. To circumvent the mutual interference between the uplink and downlink, the Frequency Division Duplex (FDD) [1] and Time Division Duplex (TDD) [1] apparatuses are commonly deployed in communication systems. In the FDD system, the uplink and downlink signals are gapped in different frequency bands, while in the TDD system, the uplink and downlink transmissions are identified in different time slots. In this way, the uplink and downlink can be treated as being orthogonal in the FDD or TDD apparatus since they utilize different frequency or time resources.

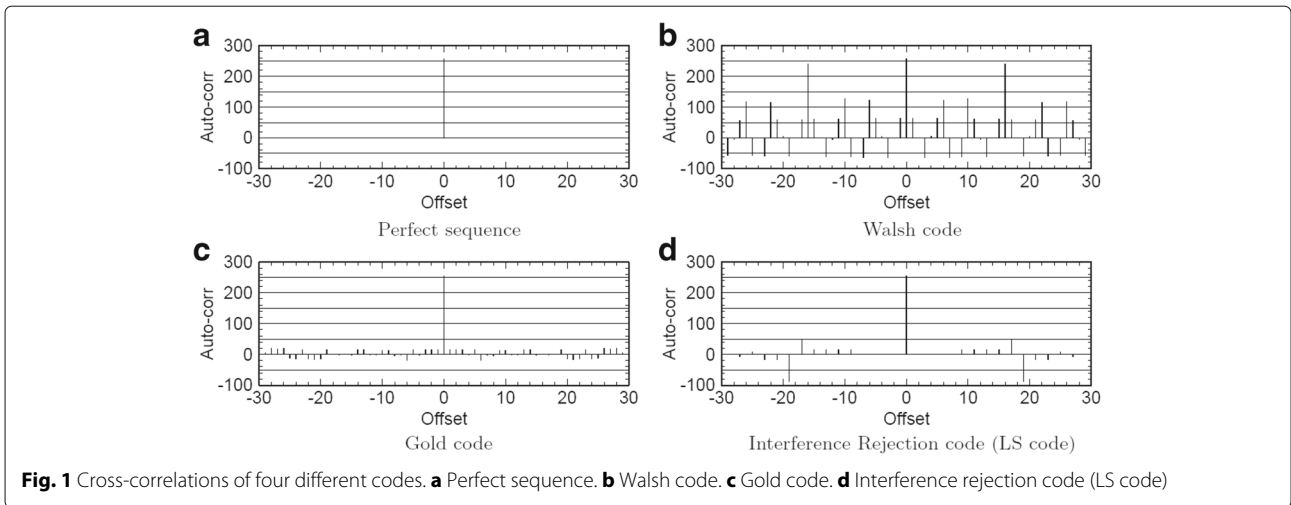
Recently, No Division Duplex (NDD) [2, 3] techniques have captured growing interests for the 5G communication system, since they can significantly increase the capacity of the cellular system as well as simplify the infrastructure of the cellular network. The basic philosophy of the No Division Duplex [2, 3] is that a radio device can transmit and receive on the same frequency at the same time; more explicitly, it can operate in a full-duplex fashion. However, as the radio signals attenuate

quickly in an exponential way over the distance, the signal from a local transmitting antenna is hundreds of thousands of times stronger than transmissions from other nodes. Therefore, the challenge in implementing a full-duplex system is to recover the desired signal from the excessively strong local interferers. Hence, a complicated interference canceller [3] must be deployed in the NDD device to combat the local interference, in both the analog RF component as well as the digital baseband component.

In Code Division Multiple Access (CDMA) systems, the spreading sequences characterize the properties of the associated Intersymbol Interference (ISI) as well as the Multiple Access Interference (MAI) [4]. Traditional spreading sequences, such as m -sequences [4], Gold codes [4], and Kasami codes [4], exhibit non-zero off-peak auto-correlations and cross-correlations, which result in a high MAI in the system. To circumvent this issue, the ideal solution is to design the optimal sequences whose auto- and cross-correlations are zero for the infinite code offsets, as shown in Fig. 1a. However, this kind of perfect sequence does not exist in theory. Therefore, considerable research has been invested on the interference rejection code which can exhibit zero correlation values on the relative delay-induced code offsets. The area which has the value of zero correlation is the so-called Zero Correlation Zone (ZCZ) or Interference-Free Window (IFW) of the spreading code [5], as shown in Fig. 1d. The auto- and

*Correspondence: weihua@cuit.edu.cn

²Chengdu University of Information and Technology, Chengdu, China
Full list of author information is available at the end of the article



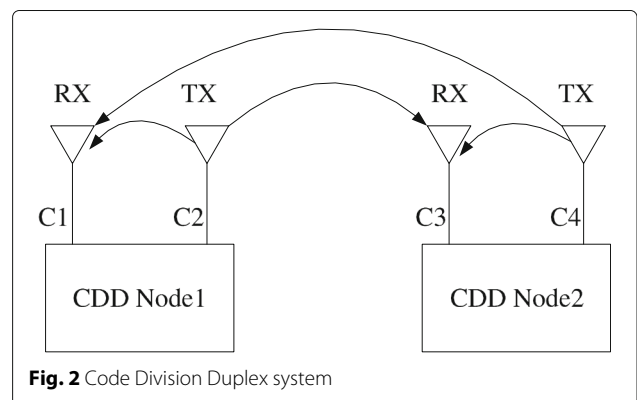
cross-correlation properties of four spreading codes are exhibited in Fig. 1. In this figure, we can observe that the correlation value of the interference rejection code is zero in IFW. Loosely Synchronous (LS) code [6, 7] is one of these specific interference rejection codes which exhibit an IFW, where the off-peak values of aperiodic auto- and cross-correlations are zero, resulting in zero ISI and zero MAI in the IFW. Given these conditions, a major benefit of the interference rejection codes is that they are capable of combating the mutual interference between the uplink and downlink without a complicated interference canceller. Hanzo, Wei, and Ni [8–10] investigated the performance of the CDMA system in the context of the deployment the LS codes. However, in their work, the power control [11] scheme is employed to avoid the near-far effect, and only the cellular communication scenarios are evaluated in previous work. In [9, 12], the interference rejection codes are deployed in the multi-carrier CDMA system and the performance is analyzed. The authors in [13] investigated the performance of the CDMA system in conjunction with the multiple antenna technique and the interference rejection code. Various chip waveforms [14] are investigated for the LS codes, and the network capacity in the cellular scenario is analyzed in [15].

In this paper, to circumvent the implementation of complicated interference canceller, Code Division Duplex (CDD) is proposed for a synchronous communication system. As shown in Fig. 2, the basic concept of the CDD is that the downlink and uplink signals are distinguished by their unique spread sequence C_i , i.e., the CDD radio can transmit and receive simultaneously at the same frequency band with different spreading signatures. The *state of the art* CDD device can operate in the same fashion as the NDD device. However, the advantage of the CDD receiver is to employ a simple matched filter or RAKE receiver rather than a complicated

interference canceller in the NDD device owing to the cross-correlation properties of the interference rejection code, which is beneficial in the engineering implementation and power saving.

In this paper, we will investigate the performance of CDD communication systems in the context of two practical scenarios. The first scenario is a cellular-like communication system, where a base station node operates as the centric node and all the other CDD nodes must communicate with the center node. In this specific scenario, the center node has a much stronger transmission power than other nodes. The second scenario is an ad hoc communication system where each CDD device transmits on the same power in the network and can communicate with each other. In this contribution, we will investigate the Bit Error Rate (BER) performance and capacity of CDD systems in both scenarios when communicating over a Nakagami- m channel.

This paper is organized as follows. In Section 2, we will introduce the specific interference rejection code, namely LS code, while in Section 3, we will describe the model



of the CDD system and fading channel. In Section 4, we will characterize the BER performance of the CDD communication, and in Section 5, we will discuss our findings. Finally, in Section 6, we will offer our conclusion.

2 Interference rejection codes

There exists a specific family of spreading codes, which exhibit an IFW; more specifically, Loosely Synchronized (LS) codes [6] exploit the properties of the so-called orthogonal complementary sets [6, 7]. Since the detailed construction method of binary LS codes was described in [6, 9, 10], here, we only focus our attention on the properties and the applications of the LS codes [16, 17].

Generally, an LS code can be denoted as $LS(N, P, W_0)$, which denotes the family of LS codes generated by applying a $(P \times P)$ -dimensional Walsh-Hadamard (WH) matrix to an orthogonal complementary code set of length N and inserting W_0 number of zeros between two orthogonal complementary sets [6, 9, 10]. The constructed $LS(N, P, W_0)$ codes can be constructed for any arbitrary length of the codes by selecting the proper parameter N , and then, the generated LS codes can exhibit an IFW of interference rejection code as shown in Fig. 1; more explicitly, the spreading signature function $c_i(t), c_j(t)$ of the constructed LS codes satisfy:

$$\int_{-\infty}^{-\infty} c_i(t)c_j(t-\tau)dt = 0, \quad \tau < W_I, \quad i \neq j \quad (1)$$

where $c_i(t)$ and $c_j(t)$ are the signature functions in the generated $LS(N, P, W_0)$ code set and W_I is the width of the IFW. More explicitly, the constructed $LS(N, P, W_0)$ codes are still orthogonal to each other even in the scenarios of the multipath environment provided that the delay spread of the multipath is less than the width of IFW. Hence, the LS code with inherent IFW can effectively suppress the Multipath Interference (MPI) and multiuser access interference (MAI), which also significantly simplify the design of receiver as well as reduce the complexity of the receiver in CDMA system.

For example, the $LS(N, P, W_0)$ codes can be generated based on the complementary pair of [6, 16], and the total number of available codes in the family of $LS(N, P, W_0)$ is given by NP . The total number of NP codes can be classified by N sets of P number of LS codes through their Walsh-Hadamard Matrix, and each set has P number of LS codes. The LS codes in the same set exhibit an IFW length of $[-W_I, +W_I]$, where we have $W_I = \min\{W_0, N - 1\}$. The aperiodic auto-correlation and cross-correlation function $\rho_{kk}(\tau), \rho_{jk}(\tau)$ of the codes belonging to the same set will be zero, provided that we have $\tau \leq W_I T_c$. Furthermore, the LS codes belonging to the N different sets are still orthogonal to each other at zero offset, namely in a perfectly synchronous environment. However, the LS

codes belonging to the N different sets will lose their orthogonality, when they have a non-zero code offset.

To combat the interference incurred by its own transmission, the spreading codes in the CDD device have the following assignment policy: the spreading codes of the uplink and downlink are wisely chosen to belong to different sets of Walsh-Hadamard. The benefit of this assignment is that the spreading codes between the uplink and downlink have the maximum width of the IFW, which can guarantee the orthogonality between the uplink and downlink in one CDD node so that their mutual interference can be negligible.

3 System model

3.1 System model

Assume that the system supports K synchronous users and each user is assigned two unique spreading signature waveforms for its uplink and downlink, respectively. The spreading signature waveform can be noted as $\mathbf{c}_k(t) = \sum_{i=0}^{G-1} c_{ki} \psi_{T_c}(t - iT_c)$, where G is the spreading gain and $\psi_{T_c}(t)$ is the rectangular chip waveform, which is defined over the interval $[0, T_c)$. Consequently, when the K users' signals are transmitted over the frequency-selective fading channel, the complex low-pass equivalent signal received at a given RX antenna can be expressed as:

$$R(t) = \sum_{k=1}^K \sum_{l=0}^{L_p-1} \sqrt{2P_k} \mathbf{c}_k(t - lT_c - \tau_k) b_k(t - lT_c - \tau_k) \times h_{kl} \exp(j\theta_{kl}) + N(t), \quad (2)$$

where $N(t)$ is the complex-valued low-pass-equivalent AWGN (additive white Gaussian noise) having a double-sided spectral density of N_0 and τ_k is the propagation delay between the transmitter and receiver for user k . In the same CDD device, τ_k is assumed to be 0, while in different CDD devices, τ_k is determined by the propagation distance: without loss of generality, $\tau_k = \frac{d_k}{c}$, where c is the speed of light. L_p is the total number of resolvable paths. P_k is the received power, which is determined by the large-scale fading of the wireless channel.

3.2 Wireless large-scale fading model

The complexity of wireless signal propagation makes it difficult to obtain a single model that characterizes path loss accurately across a range of different environments. In the textbook [1], various propagation models of the wireless channel are proposed and investigated in wireless communications, such as the well-known free-space channel model, Okumura Model [1], Hata Model [18], and COST207 [1, 18] which are traditionally used in system analysis. However, for the convenience of analysis of various system performance, we simplify the channel model as well as capture the essence of signal propagation without

resorting to complicated path loss models, which is sufficiently accurate to approximate the real channel model. In this contribution, the following simplified models [1] for path loss as a function of distance are commonly used for system design:

$$P_r = P_t G_a \left[\frac{d}{d_0} \right]^{-\gamma}, \quad (3)$$

where d_0 is the wavelength of the radio signal, d is the distance between the transmitter and receiver, and G_a is the constant which is related to the characteristic of the antenna, such as the height and direction. Parameter γ is the exponential attenuation factor which is related to the practical environment. Generally, the attenuation factor γ is about 2 to 4 according to the free-space, indoor, urban, or hilly environments.

3.3 Channel model

The DS-CDMA signal experiences independent frequency-selective Nakagami- m fading. The complex low-pass equivalent representation of the Channel Impulse Response (CIR) encountered by the k th user is given by [19]:

$$h_k(t) = \sum_{l=0}^{L_p-1} h_{kl} \delta(t - lT_c) \exp(j\theta_{kl}), \quad (4)$$

where h_{kl} represents the Nakagami-distributed fading envelope, lT_c is the relative delay of the l th path of user k with respect to the main path, while L_p is the total number of resolvable multipath components. Furthermore, θ_{kl} is the uniformly distributed phase-shift of the l th multipath component of the channel and $\delta(t)$ is the Kronecker delta function. More explicitly, the L_p multipath attenuations $\{h_{kl}\}$ are independent Nakagami-distributed random variables with a Probability Density Function (PDF) of [20–22]:

$$p(h_{kl}) = M(h_{kl}, m_{kl}, \Omega_{kl}),$$

$$M(R, m, \Omega) = \frac{2m^m R^{2m-1}}{\Gamma(m)\Omega^m} e^{(-m/\Omega)R^2}, \quad (5)$$

where $\Gamma(\cdot)$ is the gamma function [19] and m_{kl} is the Nakagami- m fading parameter, which characterizes the severity of the fading for the l th resolvable path of user k [23]. Specifically, $m_{kl} = 1$ represents Rayleigh fading, $m_{kl} \rightarrow \infty$ corresponds to the conventional Gaussian scenario, and $m_{kl} = 1/2$ describes the so-called one-sided Gaussian fading, i.e., the worst-case fading condition. The Rician and log-normal distributions can also be closely approximated by the Nakagami distribution in conjunction with values of $m_{kl} > 1$. The parameter Ω_{kl} in Eq. 5 is the second moment of h_{kl} , i.e., we have $\Omega_{kl} = E[(h_{kl})^2]$. We assume a negative exponentially decaying Multipath Intensity Profile (MIP) given by $\Omega_{kl} = \Omega_{k0} e^{-\eta l}$, $\eta \geq 0, l =$

$0, \dots, L_p - 1$, where Ω_{k0} is the average signal strength corresponding to the first resolvable path and η is the rate of average power decay.

4 BER performance analysis

As shown in Fig. 3, let the first user be the user of interest and consider a receiver using de-spreading as well as multipath diversity combining. The conventional matched filter-based RAKE receiver using maximum ratio combining (MRC) can be invoked for detection, where we assume that the RAKE receiver combines a total of L_r number of diversity paths, which may be more or possibly less than the actual number of resolvable components at the current chip rate. It is advocated that the system has achieved perfect time synchronization and perfect estimates of the channel tap weights. Then, after appropriately delaying the outputs of the individual matched filter, in order to coherently combine the L_r number of path signals with the aid of the RAKE receiver, the output Z_{kl} of the RAKE receiver's l th finger sampled at $t = T + lT_c + \tau_k$ can be expressed as:

$$Z_{kl} = D_{kl} + I_{kl}, \quad (6)$$

where D_{kl} represents the desired direct component, which can be expressed as:

$$D_{kl} = \sqrt{2PT_s} b_k[0] h_{kl}^2, \quad (7)$$

where T_s is the symbol duration.

The MRC's decision variable Z_k , which is given by the sum of all the RAKE fingers' outputs, can be expressed as:

$$Z_k = \sum_{l=0}^{L_r-1} Z_{kl}. \quad (8)$$

The RAKE fingers' output signal Z_{kl} is a Gaussian distributed random variable with a mean of D_{kl} .

The term I_{kl} in Eq. 6 represents the total interference incurred by the Multipath Interference (MPI) as well as the Multiple Access Interference (MAI), which can be expressed as:

$$I_{kl} = I_{kl}[S] + I_{kl}[M] + N_k, \quad (9)$$

where $I_{kl}[S]$ represents the multipath interference imposed by the user of interest, which can be expressed as:

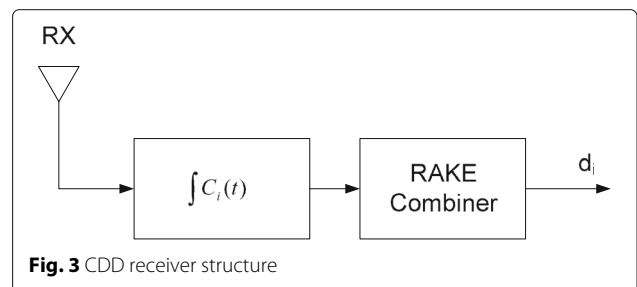


Fig. 3 CDD receiver structure

$$I_{kl}[S] = \sqrt{2PT_s}h_{kl} \sum_{\substack{l_p=0 \\ l_p \neq l}}^{L_p-1} \frac{h_{kl_{l_p}} \cos \theta_{kl_{l_p}}}{T_s} \times \int_0^{T_s} b_k [t - (l_p - l) T_c] \cdot c [t - (l_p - l) T_c] c[t] dt. \quad (10)$$

Furthermore, $I_{kl}[M]$ represents the multiuser interference inflicted by the $K - 1$ number of interfering signals, which can be expressed as:

$$I_{kl}[M] = \sqrt{2PT_s}h_{kl} \sum_{\substack{k'=1 \\ k' \neq k}}^K \sum_{l_p=0}^{L_p-1} \frac{h_{k'l_p} \cos \theta_{k'l_p}}{T_s} \cdot \int_0^{T_s} b_{k'} [t - (l_p - l) T_c - (\tau_{k'} - \tau_k)] \times c_{k'} [t - (l_p - l) T_c - (\tau_{k'} - \tau_k)] c[t] dt. \quad (11)$$

In Eqs. 10 and 11, the $\cos(\cdot)$ terms are contributed by the phase differences between the incoming carrier and the locally generated carrier used in the demodulation. Finally, the noise term in Eq. 9 can be expressed as:

$$N_{kl} = h_{kl} \int_0^{T_s} n(t)c[t] \cos(2\pi f_c t + \theta_{kl}) dt, \quad (12)$$

which is a Gaussian random variable with a zero mean and a variance of $N_0 T_s h_{kl}^2$, where $\{h_{kl}\}$ represents the path attenuations.

Furthermore, $I_{kl}[S]$ represents the MPI imposed by the user of interest. Without loss of generality, we can assume that the width of the IFW is longer than the channel spread time $L_p T_c$, and in this case, the MPI becomes zero since the auto-correlation of the spreading code is zero.

Hence, the performance of the CDD system is mainly determined by the MAI term $I_{kl}[M]$, which is affected by channel delay profile, distance amongst the nodes, and the number of users supported in a cell.

Again, the uplink TX and downlink RX have different spreading sequences for the k th user in one CDD device, and recall that the system can assign different sets of the spreading codes for the uplink and downlink; more specifically, the spreading codes of the uplink and downlink have the maximum width of IFW in the generated LS codes. And the distance between the TX antenna and RX antenna is very close, i.e., $\tau_k = 0$. Hence, after the matched filter and RAKE receiver, the interference introduced by its own transmission can be ignored due to the inherent orthogonality of the spreading codes. Thus, the MAI are mainly introduced by other CDD device nodes.

Since the power control is difficult to be implemented in the CDD system, the near-far effect must be taken into account for the BER performance analysis. Assume that the power of the interested signals is P_k while the power

of the interference is P_j , and P_k and P_j can be obtained from Eq. 3.

As shown in Fig. 4, if one path of the channel impulse response of the interference user is located within the IFW, this specific path will not introduce any interference to the interested signals. More explicitly, only these paths which are located outside the interference-free window will introduce the MAI to the desired signal. Without loss of generality, we can assume that the multipath intensity profile of all users obeys the same distribution, i.e., $\Omega_{k0} = \Omega_0, k = 1, 2, \dots, K$, and $E_b = PT_s$ is the energy per bit. Thus, the variance of the l th RAKE finger's output samples Z_{kl} for a given set of channel amplitudes $\{h_{kl}\}$ may be approximated as [23, 24]:

$$\sigma_{kl}^2 = 2PT_s^2 \left[\frac{\chi_{kl}}{3G} + \left(\frac{2\Omega_0 E_b}{N_0} \right)^{-1} \right] \cdot \Omega_0 h_{kl}^2, \quad (13)$$

$$\chi_{kl} = \sum_{j=1}^K \sum_{l=0}^{L_p-1} \frac{P_j}{P_k} e^{-\eta^l} u(W_I - |\tau_j - \tau_k| - l) \quad (14)$$

where W_I is the width of the IFW; τ_j and τ_k are the propagation delay of the interference user j and the interested user k , respectively; L_p is the total number of resolvable paths; and $u(x)$ is the step function, i.e., $u(x) = 1, x \geq 0$, otherwise $u(x) = 0, x < 0$. According to the large-scale fading model, P_j and P_k are the strength of the received signals, which can be derived in Eq. 3 as $P_j = P_{tj} G_a \left[\frac{d_j}{d_0} \right]^{-\gamma}$, $P_k = P_{tk} G_a \left[\frac{d_k}{d_0} \right]^{-\gamma}$. Moreover, the propagation delay obeys $\tau_j = d_j/c$, $\tau_k = d_k/c$.

Hence, the MRC's output sample Z_k can be approximated by a Gaussian random variable with a mean of

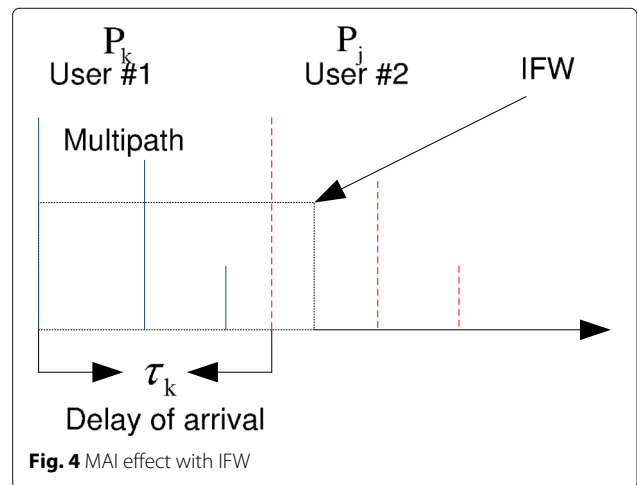


Fig. 4 MAI effect with IFW

$E[Z_k] = \sum_{l=0}^{L_r-1} D_{kl}$ and a variance of $\text{Var}[Z_k] = \sum_{l=0}^{L_r-1} \sigma_{kl}^2$ [21, 24], where we have:

$$E[Z_k] = \sum_{l=0}^{L_r-1} \sqrt{2PT_s} b_k[0] h_{kl}^2, \quad (15)$$

$$\text{Var}[Z_k] = \sum_{l=0}^{L_r-1} \sigma_{kl}^2. \quad (16)$$

Hence, the BER using BPSK modulation conditioned on a set of fading attenuations $\{h_{kl}, l = 0, 1, \dots, L_r - 1\}$ can be expressed as [1, 18]:

$$P_b(\gamma) = Q\left(\sqrt{\frac{E[Z_k]}{\text{Var}[Z_k]}}\right) = Q\left(\sqrt{\sum_{l=0}^{L_r-1} 2\gamma_l}\right), \quad (17)$$

where $Q(x)$ represents the Gaussian Q-function which can also be simplified as [1, 23]:

$$Q(x) = \frac{1}{\pi} \int_0^{\pi/2} \exp\left(-\frac{x^2}{2 \sin^2 \theta}\right) d\theta, x \geq 0. \quad (18)$$

Furthermore, $2\gamma_l$ in Eq. 17 represents the output Signal to Interference plus Noise Ratio (SINR) at the l th finger of the RAKE receiver.

Let us now substitute Eqs. 13, 15, and 16 into Eq. 17, and the expressions under the square-root functions must be equal, which allows us to express γ_l as follows:

$$\gamma_l = \left[\frac{\chi_{kl}}{3G} + \left(\frac{\Omega_0 E_b}{N_0}\right)^{-1} \right]^{-1} \cdot \frac{h_{kl}^2}{\Omega_0}. \quad (19)$$

For the convenience of the BER derivation, we define a term γ_c as:

$$\gamma_c = \left[\frac{\chi_{kl}}{3G} + \left(\frac{\Omega_0 E_b}{N_0}\right)^{-1} \right]^{-1}. \quad (20)$$

With the aid of Eq. 20, we have $\gamma_l = \gamma_c \cdot \frac{(h_l)^2}{\Omega_0}$ and h_l obeys the Nakagami- m distribution characterized by Eq. 5, and the PDF of γ_l can be formulated as:

$$p_{\gamma_l}(\gamma_l) = \left(\frac{m_l}{\bar{\gamma}_l}\right)^{m_l} \frac{\gamma^{m_l-1}}{\Gamma(m_l)} \exp\left(-\frac{m_l \gamma_l}{\bar{\gamma}_l}\right), \quad \gamma_l \geq 0, \quad (21)$$

where $\bar{\gamma}_l = \gamma_c e^{-\eta l}$ for $l = 0, 1, \dots, L_r - 1$. The average BER, $P_b(E)$, can be obtained by the weighted averaging of the conditional BER expression of Eqs. 17 and 21 over the joint PDF of the instantaneous SNR values.

5 Simulation performance of CDD

As we mentioned before, two scenarios are investigated in this paper. The first scenario is a cellular system which has a center node, and all other nodes besides the center node only communicate with the center one. The second scenario is a relay and ad hoc communication environment,

where any two of the nodes can communicate with each other. For the CDD performance evaluation, we assume that the system has a chip rate of 1.2288 M chips which is the same as the CDMA2000 and EVDO systems [25]. The bandwidth of our system is 1.25 MHz. The carrier frequency of the system is $f_c = 2$ GHz, and the large-scale fading factor $\gamma = 2.5$. Moreover, the radius of a cell is configured to 2000 m. All the CDD nodes are operated in synchronous transmission mode, i.e., all nodes transmit simultaneously. We also assume that the maximum delay spread of the channel is $\tau = 3 \mu s$ [11]. Thus, the number of resolvable paths is considered as $L_p = \lfloor \frac{\tau}{T_c} \rfloor + 1 = 4$, where $\tau = 3 \mu s$, and the channel's delay spread profile is negatively exponentially distributed with the factor η in the range of $[0.3, 3] \mu s$. The RAKE receiver combines $L_r = 3$ number of fingers for BER performance evaluation, and the channel's exponential decay factor is $\eta = 0.2$.

In our simulation, the LS(4,32,4) codes are deployed as the spreading codes. More explicitly, the total length of the LS(4,32,4) code is $L = NP + 2W_0 = 136$ chips, and its spreading factor may be calculated by simply noting that each bit to be transmitted is spread by one of the constituent LS(4,32,4) codes. Although the length of this LS code is $L = NP + 2W_0 = 136$, the effective spreading gain of the LS code is identical to $G_{\text{eff}} = 128$ since the inserting zeros must not be taken into account. The LS(4,32,4) codes are constituted by a total of 128 spreading codes. The width of the IFW W_I and the number of supported user K satisfies that:

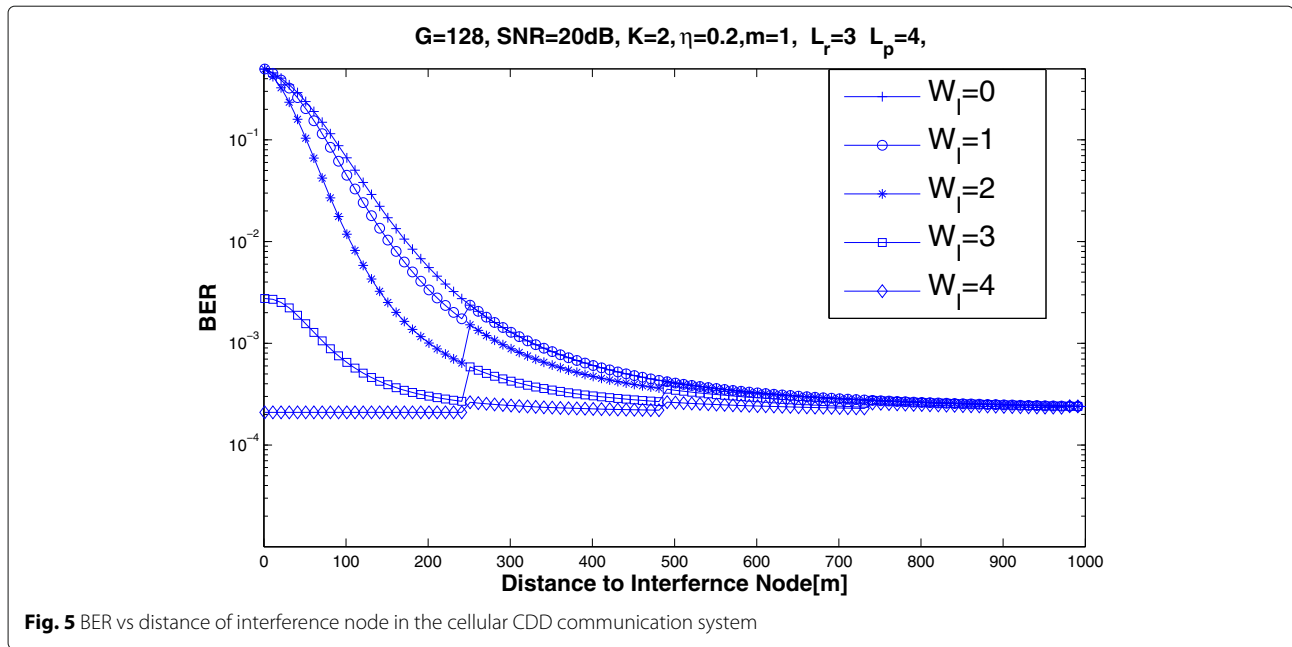
$$W_I = 4, K \leq 16;$$

$$W_I = 2, 16 < K \leq 32;$$

$$W_I = 1, 32 < K \leq 64;$$

$$W_I = 0, 64 < K \leq 128.$$

First, we investigated the BER performance of CDD when there existed a strong interference CDD node. In this scenario, a cell has three CDD nodes, the source node, the destination node, and the interference node. In our simulation, the interference node has a transmission power 20 dB higher than the source node. It is obvious that the distance between the interference node and destination node dramatically affects the performance of the RAKE receiver since the strength of interference is inversely proportional to the distance. Figure 5 exhibits the BER performance of the destination node in conjunction with the distance between the interference node and destination node. More explicitly, we can observe that when the width of IFW W_I is below 2 and the distance of the interference node is less than 300 m, the effect of the interference node cannot be completely rejected by the interference spreading code so that the MAI leak inevitably in the RAKE receiver due to the insufficient width of the IFW. However, when the W_I increases to 3

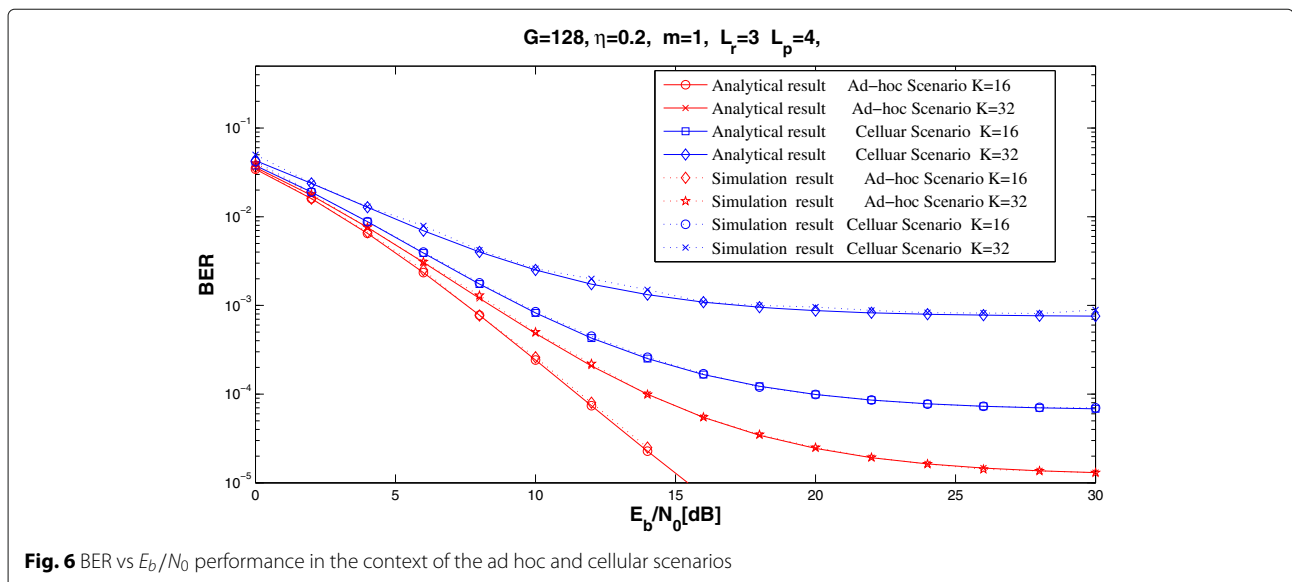


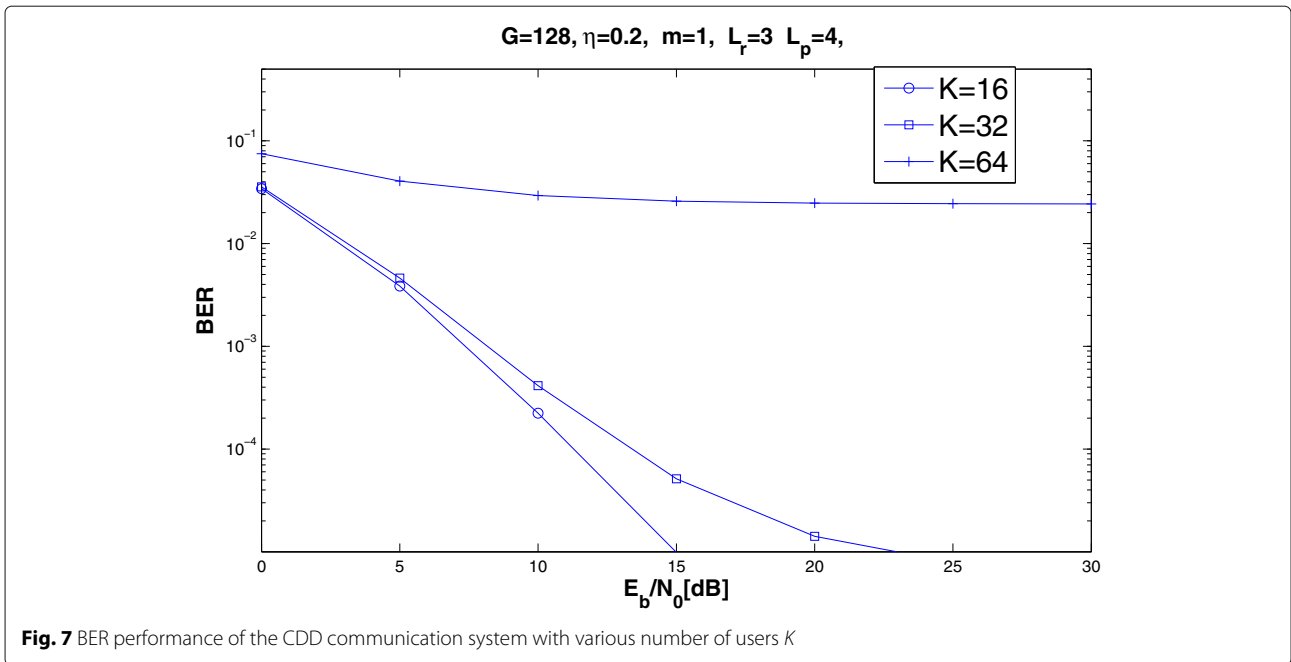
or 4, the interference is suppressed significantly and the effect of the interference node is negligible.

The performance of CDD in two common scenarios is shown in Fig. 6. In the cellular scenario, a center node or Base Station (BS) exists in the network, which has a high transmission power than other nodes. In our simulation, we assume that the base station node has a 20-dB higher transmission power. The second is an ad hoc scenario where each node has the same transmission power. Figure 6 plots the BER performance of the CDD communication system in the context of a various number of users K . In Fig. 6, we can observe that the performance

in the ad hoc scenario is superior than that in the cellular scenario. This phenomenon is reasonable since the cellular environment exists as a strong base station which also acts as a strong interference node to other destination nodes and then degrades the BER performance in the cellular condition.

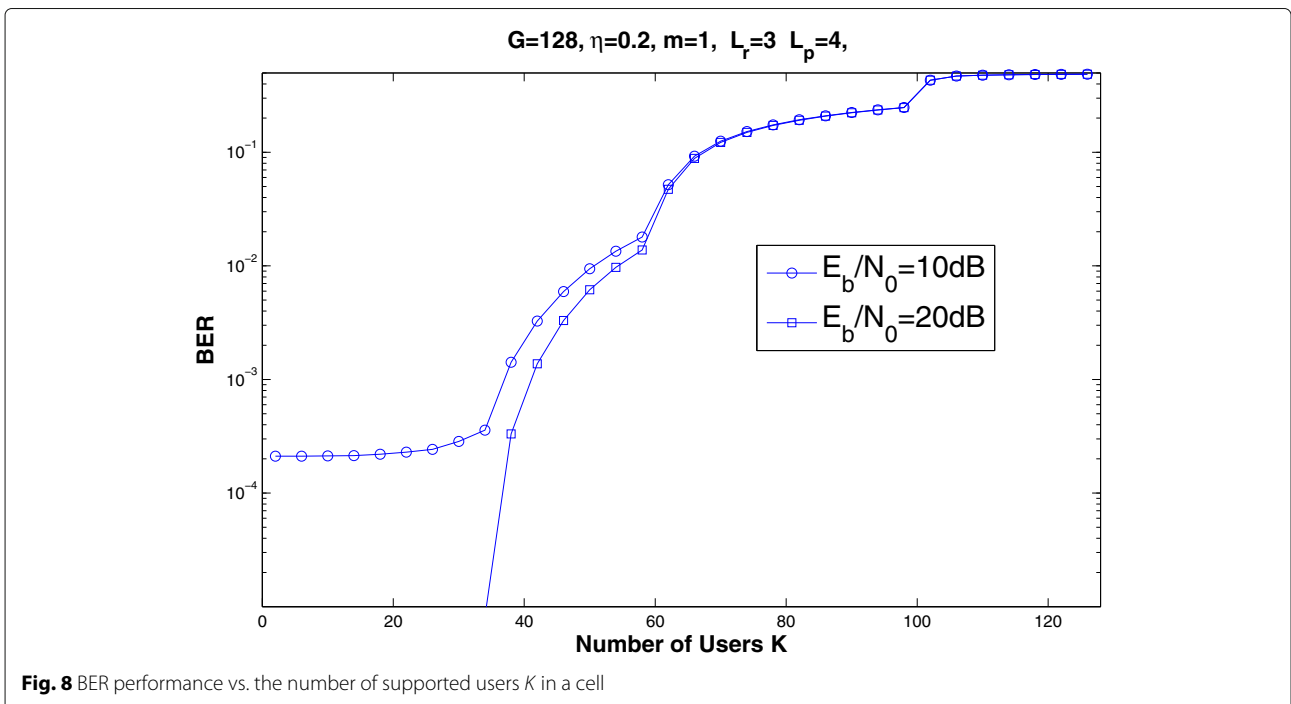
Figures 7 and 8 exhibit the performance of the CDD system in conjunction with various supported users K . From Fig. 7, we can observe that the near interference-free performance can be achieved when the number of users K is less than 16 since the spreading codes have the maximum width of the IFW in this condition. As





the number of users is increased to 32, the performance of the CDD system is degraded moderately, since the width of the IFW is still maintained in $W_I \leq 2$. However, when the number of users is increased to more than 64, the performance is degraded significantly since the width of IFW is decreased to $0 \sim 1$, which reduces the capability of combating the MAI. Figure 8 portrays the

BER performance of the CDD in conjunction with various users K . Two different SNR parameters are configured in our simulation, i.e., SNR = 10 dB and SNR = 20 dB, respectively. From Fig. 8, we can conclude that the CDD system exhibits a near interference-free performance in the case $K \leq 32$. In Figs. 7 and 8, it is advocated that the CDD system should be deployed in a relatively-low



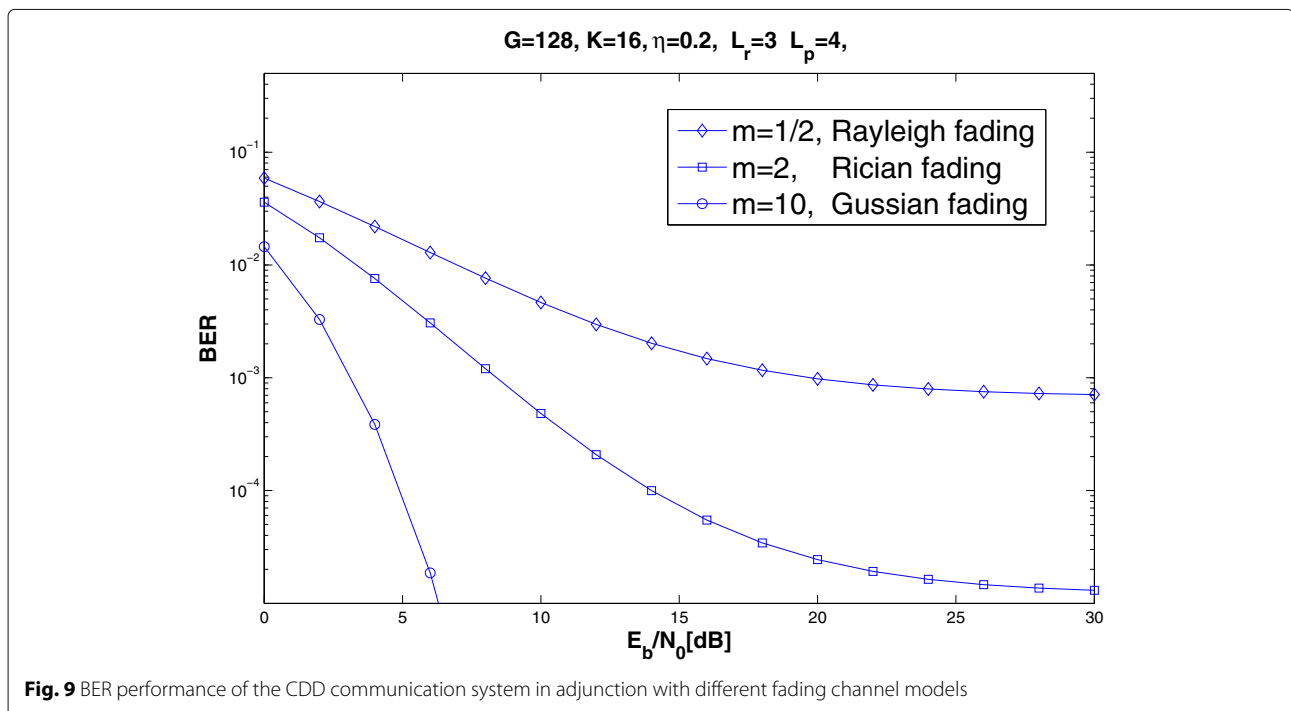
load of users. For a spreading gain of 128 systems, the CDD system can support $K = 40$ user communications simultaneously without the mutual interference; this load is promising since the linear Minimum Mean Square Estimator (MMSE) multiuser detector with a much higher complexity can only support to $K = 40$ to achieve an ideal performance. Similarly, the performance of the linear MMSE multiuser detector [26, 27], the Parallel Interference Canceller (PIC) [26, 27], and Serial Interference Canceller (SIC) [26, 27] deteriorates significantly for the high load scenario in a CDMA system; furthermore, the traditional MMSE detector, PIC, and SIC suffer the serious near-far effect and degrade the performance in our CDD scenarios. The ideal Maximum Likelihood detector [26, 27] can solve this issue; however, the complexity of the ML detector is excessively high so that it is impossible to implement in practical communication systems.

Finally, Fig. 9 plots the BER performance of different channel fading models. The Nakagami- m channel is a generic model for the wireless channel, where the choice of the parameter m determines the fading type of the channel model. In Fig. 9, three different fading models are simulated and analyzed in our investigation. More explicitly, the Rayleigh fading [1, 18], Rician fading [1, 18], and Gaussian Fading [1, 18] are evaluated in the simulation. In the practical applications in a cellular communication, the Rayleigh fading and Rician fading model are commonly adopted for the performance evaluation. Hence, in this detection, we evaluate the CDD performance in

conjunction with the real scenario of the cellular communications. The simulation results in Fig. 9 conform to the mathematic analysis, and we can conclude that the performance of Rayleigh fading is the worst and the performance of Gaussian fading is the best amongst these three fading models.

6 Conclusions

In this paper, we investigated the BER performance of the CDD communication system, which can exhibit the same operation fashion as the NDD device. Moreover, the advantage of the CDD is that the receiver can be simplified as the matched filter or RAKE receiver by carefully selecting our proposed interference rejection codes—LS codes. Hence, our proposed method can significantly reduce the complexity and difficulty in the implementation of the NDD fashion. Our simulation results show that the CDD system can achieve a near interference-free performance in a low-user load scenario due to the limited number of available LS codes having a certain IFW width; more explicitly, our simulation and analysis show that the CDD system can achieve an ideal performance when the number of user $K \leq 32$, and in this condition, a simple matched filter or RAKE receiver is sufficient to combat all the interference. For future research, the method of the smart assignment of the spreading codes will be investigated to reduce interference between neighboring nodes and increase the capacity and spectrum efficiency of the CDD network.



Acknowledgements

This work is supported by the Scientific Research Foundation of Chengdu Technological University (grant no. 2017RC004) and the Scientific Research Foundation of CUIT (KYTZ201501, KYTZ201502); the Sichuan Provincial Department of Science and Technology in granted program nos. 2015GZ0340, 2015GZ0286, 2015GZ0290, and 2015RZ0060; and the National Defense Innovation Technology Program 173-162-11-ZT-003-012-02. Finally, great thanks to the anonymous reviewers for their valuable suggestions to improve the quality of this paper.

Funding

The work is sponsored by Chengdu Technological University (grant no. 2017RC004); Chengdu University of Information and Technology (KYTZ201501, KYTZ201502); Sichuan Provincial Department of Science and Technology in granted program nos. 2015GZ0340, 2015GZ0286, 2015GZ0290, and 2015RZ0060; and the National Defense Innovation Technology Program 173-162-11-ZT-003-012-02.

Authors' contributions

YY and HW contributed to the conception and design of the study. YY, LL, GL, and HW contributed to the acquisition of data and simulation. YY, GL, LL, and HW contributed to the analysis and interpretation of the simulation data. All authors read and approved the final manuscript.

Authors' information

Dr. Yufang Yin obtained her Ph.D. degree in 2007 from the EE department, the University of Texas at San Antonio. From January 2009 to June, 2012, she worked as the specialist and research scientist in Nokia Networks. From July 2012 to October 2014, she worked as the staff engineer in Spread Spectrum Communication. Since November 2016, she joined Chengdu Technological University. Her research area includes statistical signal processing and applied machine learning.

Gangjun Li received the B.S. degree in Mechanical Engineering from the University of Electronic Science and Technology of China in 1987 and the M.S. degree in Mechanics from the Harbin Institute of Technology in 1990. He received the Ph.D. degree in Robotics Engineering from the Southwest Jiaotong University in 2002. Since 2010, he is a professor of Chengdu Technological University (CDTU). His research interests are in areas of robotics, simulation, modeling of complex systems, and nonlinear control.

Dr. Li (Alex) Li obtained his Ph.D. degree in electronics engineering from the University of York in 2014, and now he is working in Chengdu University of Information Technology, China. His research interests include fields of wireless communication, MIMO-OFDM, adaptive filtering, and ASIC design.

Hua Wei obtained his Ph.D. degree from the ECS department, University of Southampton in September 2005. From January 2006 to September 2014, he worked as the principle engineer in Spread spectrum Communication for wireless modem design. Since September 2014, he joined in Chengdu University of Information Technology. His research area includes adaptive equalization, signal processing, and VLSI design for wireless baseband processor.

Competing interests

The authors declare that they have no competing interests.

Publisher's Note

Springer Nature remains neutral with regard to jurisdictional claims in published maps and institutional affiliations.

Author details

¹Chengdu Technological University, Chengdu, China. ²Chengdu University of Information and Technology, Chengdu, China.

Received: 6 January 2017 Accepted: 24 August 2017

Published online: 04 September 2017

References

1. A Goldsmith, *Wireless communications*. (Cambridge University Press, 2005)
2. T Riihonen, S Werner, R Wichman, Mitigation of loopback self-interference in full-duplex MIMO relays. *IEEE Trans. Sign. Process.* **59**(12), 5983–5993 (2011)
3. M Duarte, C Dick, A Sabharwal, Experiment-driven characterization of full-duplex wireless systems. *IEEE Trans. Wirel. Commun.* **1**(12), 4296–4307 (2012)
4. L Hanzo, LL Yang, EL Kuan, K Yen, *Single- and multi-carrier DS-SS-CDMA*. (John Wiley and IEEE Press, 2003), p. 1060
5. P Fan, L Hao, Generalized orthogonal sequences and their applications in synchronous CDMA systems. *IEICE Trans. Fundam.* **E83-A**, 2054–2069 (2000)
6. S Stańczak, H Boche, M Haardt, in *GLOBECOM '01*. Are LAS-codes a miracle? vol. 1 (IEEE Global Telecommunications Conference, San Antonio, 2001), pp. 589–593
7. CC Tseng, CL Liu, Complementary sets of sequences. *IEEE Trans. Inf. Theory.* **18**, 644–652 (1972)
8. H Wei, L Hanzo, On the uplink performance of asynchronous LAS-CDMA. *IEEE Trans. Wirel. Commun.* **5**, 1187–1196 (2006)
9. H Wei, L-L Yang, L Hanzo, Interference-free broadband single- and multi-carrier DS-SS-CDMA. *IEEE Commun. Mag.* **43**(2), 68–73 (2005)
10. S Ni, H Wei, JS Blough, L Hanzo, Network performance of asynchronous UTRA-like FDD/CDMA systems using loosely synchronised spreading codes. *IEEE Veh. Technol. Conf.* **2**, 1359–1363 (2003)
11. WCY Lee, *Mobile communications engineering*, 2nd ed. (McGraw-Hill, New York, 2008)
12. L-L Yang, W Hua, L Hanzo, Multiuser detection assisted time- and frequency-domain spread multicarrier code-division multiple-access. *IEEE Trans. Veh. Technol.* **55**(1), 397–404 (2006)
13. H Wei, L-L Yang, L Hanzo, Downlink space-time spreading using interference rejection codes. *IEEE Trans. Veh. Technol.* **55**(6), 1838–1847 (2006)
14. H Wei, L Hanzo, in *2005 6th IEE International Conference on 3G and Beyond*. LAS-CDMA Using Various Time Domain Chip-Waveforms (IET Conference Publications, 2005)
15. X Liu, H Wei, L Hanzo, Analytical bit error rate performance of DS-SS-CDMA ad hoc networks using large area synchronous spreading sequences. *IET Commun.* **1**(4), 760–764 (2007)
16. RL Frank, Polyphase complementary codes. *IEEE Trans. Inf. Theory.* **26**, 641–647 (1980)
17. R Sivaswamy, Multiphase complementary codes. *IEEE Trans. Inf. Theory.* **24**, 546–552 (1978)
18. D Tse, P Viswanath, *Fundamentals of wireless communication*. (Cambridge University Press, 2005)
19. JG Proakis, *Digital communications*, 3rd edn. (Mc-Graw Hill International Editions, 1995)
20. N Nakagami, in *Statistical methods in radio wave propagation*, ed. by WG Hoffman. The *m*-distribution, a general formula for intensity distribution of rapid fading (Pergamon, Oxford, 1960)
21. T Eng, LB Milstein, Coherent DS-SS-CDMA performance in Nakagami multipath fading. *IEEE Trans. Commun.* **43**, 1134–1143 (1995)
22. V Aalo, O Ugweje, R Sudhakar, Performance analysis of a DS/SS-CDMA system with noncoherent *M*-ary orthogonal modulation in Nakagami fading. *IEEE Trans. Veh. Technol.* **47**, 20–29 (1998)
23. M-S Alouini, AJ Goldsmith, A unified approach for calculating error rates of linearly modulated signals over generalized fading channels. *IEEE Trans. Commun.* **47**, 1324–1334 (1999)
24. MK Simon, M-S Alouini, A unified approach to the probability of error for noncoherent and differentially coherent modulation over generalized fading channels. *IEEE Trans. Commun.* **46**, 1625–1638 (1998)
25. 3GPP2, Overviews of the CDMA2000 standards. Website: www.3gpp2.org
26. X Wang, VH Poor, *Wireless communication systems: advanced techniques for signal reception*. (Prentice Hall, 2011)
27. HV Poor, L Tong, *Signal processing for wireless communication system*. (Springer, 2012)